Droplet Nucleation and Domain Wall Motion in a Bounded Interval

Robert S. Maier[1,2] and D. L. Stein[2,1]
[1]*Mathematics and* [2]*Physics Departments, University of Arizona, Tucson, Arizona 85721*

We study a spatially extended model of noise-induced magnetization reversal: a classical Ginzburg–Landau model, restricted to a bounded interval and perturbed by weak spatiotemporal noise. By adapting the Coleman–Langer approach to false vacuum decay, we determine the dependence of the activation barrier and Kramers rate prefactor on the interval length. As it increases, a transition between activation regimes occurs, at which the prefactor diverges. Similar transitions between activation regimes should occur in many other bistable, spatially extended classical models.

PACS numbers: 05.40.-a, 05.45.Yv, 11.10.Wx, 75.60.Jk

The effect of noise on spatially extended classical-mechanical systems has become a subject of intense investigation [1]. Noise, by which is meant local fluctuations of thermal or other origin, may be spatiotemporal: it may vary randomly in space as well as time.

A typical problem is the determination of the extent to which spatiotemporal noise can induce transitions between the stable states of a system modeled by a nonlinear field equation, or induce such a system to escape from a metastable state. The dependence on system size is of especial importance. For example, the thermally activated reversal of a micromagnet is described by a spatially extended, finite-volume version of the stochastic Landau–Lifshitz–Gilbert equation [2]. The spatial extent causes magnetization reversal to differ from the 'zero-dimensional' case, where the noise has no spatial dependence [3]. Activation by spatiotemporal noise in finite volumes is also important in the formation of localized structures in electroconvection [4].

The Coleman–Langer approach to false vacuum decay [5] has been applied to transitions between stable states, in classical as well as quantum models with infinite spatial extent. For example, Braun [6](a) applied it to a model of an infinitely elongated micromagnet, and was able to compute a reversal rate per unit length. However, the original Coleman–Langer technique was not designed for systems with *finite* spatial extent.

In this Letter, we determine the effects of weak spatiotemporal noise on a finite one-dimensional system: an overdamped classical Ginzburg–Landau model, confined to the bounded interval $[0, L]$. This is a finite-size counterpart of the original model of Langer [7]. It has two stable states, of positive and negative magnetization. In the weak-noise limit, noise-activated magnetization reversals become exponentially rare, the reversal rate being given by the Kramers formula $\Gamma \sim \Gamma_0 \exp(-\Delta W/\epsilon)$. Here ϵ is the noise strength, ΔW is the activation barrier between the stable states, and Γ_0 is the rate prefactor.

This finite-size model was first studied by Faris and Jona-Lasinio [8], who worked out a 'large deviation theory' of its magnetization reversals, but did not compute the prefactor. We compute it in closed form, as a function of L. It contains a quotient of infinite-dimensional fluctuation determinants, which we evaluate with the aid of elliptic functions and elliptic integrals. Our analytic techniques are a significant advance on the original Coleman–Langer technique, which does not use higher transcendental functions, and is therefore restricted to the $L \to \infty$ limit.

We uncover a surprising result: an unusual phase transition occurring when L is increased from zero to infinity. In dimensionless units, it occurs at $L = 2\pi$ (if Dirichlet or periodic boundary conditions are imposed) or $L = \pi$ (in the Neumann case). At the critical length, the rate prefactor Γ_0 *diverges*. This is due to the bifurcation of the transition state that interpolates between the two stable states. A zero-field 'sphaleron' configuration, which serves as transition state when L is small, bifurcates into a degenerate pair of 'periodic instantons'. Similar bifurcations have been studied in nonzero-temperature quantum field theory [9,10], where the length L is chosen to equal $\hbar c/k_B T$. Until now, their relevance to classical activation by spatiotemporal noise was not understood.

In the small-L regime, activation behavior is essentially zero-dimensional. In the large-L regime, the optimal (i.e., energetically favored) state-space trajectory for magnetization reversal is quite different. If periodic boundary conditions are imposed, reversal will most likely proceed via the nucleation of a droplet within a pair of Bloch walls; but in the Dirichlet and Neumann cases, a single wall will form at $x = 0$ or $x = L$, and sweep across the interval.

In a model of a one-dimensional micromagnet undergoing field-induced magnetization reversal, a comparable transition between activation regimes is present [6](b). We predict that many other spatially extended models incorporating weak spatiotemporal noise, such as models of electroconvection, will display similar phase transitions. As the size of the spatial domain moves through a critical value separating two activation regimes, the activation rate prefactor should diverge or otherwise become singular.

Model and Phenomenology.—Following Faris and Jona-Lasinio [8], we consider on $[0, L]$ a classical field $\phi = \phi(x, t)$ that evolves according to the stochastic Ginzburg–Landau equation

$$\dot{\phi} = M\phi'' + \mu\phi - \lambda\phi^3 + \epsilon^{1/2}\xi(x, t), \tag{1}$$

where $\xi(x, t)$ is unit-strength spatiotemporal white noise, satisfying $\langle \xi(x_1, t_1)\xi(x_2, t_2)\rangle = \delta(x_1 - x_2)\delta(t_1 - t_2)$. We set

$M = \mu = \lambda = 1$, or equivalently use dimensionless units, in which the length unit is the nominal coherence length $\sqrt{M/\mu}$, the field strength unit is $\sqrt{\mu/\lambda}$, etc.

In the absence of noise, the time-independent solutions of (1) include the sphaleron $\phi \equiv 0$, and $\phi \equiv \pm 1$; the latter are the magnetized states in the Neumann and periodic cases. In the Dirichlet case, $\phi(x = 0) = \phi(x = L) = 0$ is imposed, so the magnetized states necessarily differ. It is easy to check that if $\epsilon = 0$, the so-called periodic instanton $\phi = \phi_{\mathrm{inst},m}(x)$ is a time-independent solution of (1) for any m in the range $0 < m \leq 1$. Here (cf. [11])

$$\phi_{\mathrm{inst},m}(x) \equiv \sqrt{\frac{2m}{m+1}}\,\mathrm{sn}(x/\sqrt{m+1} \mid m), \qquad (2)$$

where $\mathrm{sn}(\bullet \mid m)$ is the Jacobi elliptic function with parameter m, which has quarter-period equal to the first complete elliptic integral $\mathbf{K}(m)$ [12]. This quarter-period decreases to $\pi/2$ as $m \to 0^+$, in which limit $\mathrm{sn}(\bullet \mid m)$ degenerates to $\sin(\bullet)$, and it increases to infinity as $m \to 1^-$. One would expect the Dirichlet-case stable magnetized states to be $\pm\phi_{\mathrm{inst},m_{s,D}}$, with $m_{s,D}$ determined implicitly by the condition $\phi(x = L) = 0$, i.e., by the half-period condition $2\sqrt{m_{s,D}+1}\,\mathbf{K}(m_{s,D}) = L$. However, this is so only if $L > \pi$. If $L \leq \pi$, there is no solution for $m_{s,D}$ in the range $0 < m_{s,D} \leq 1$, and the Dirichlet-case model is monostable with the zero-field configuration as its stable state, rather than bistable.

Noise-activated magnetization reversal, for weak noise, proceeds with high likelihood along an optimal trajectory in the model's infinite-dimensional state space that goes 'uphill' from a magnetized state to an intermediate transition state. In a zero-dimensional approximation, this is the $\phi \equiv 0$ sphaleron. However, on physical grounds one expects a transition state to be a unstable 'droplet pair' field configuration, in which half the interval is occupied by each magnetization value. Mathematically, this can arise as follows. In the Dirichlet case, $\phi \equiv 0$ undergoes a pitchfork bifurcation into the degenerate magnetized states $\pm\phi_{\mathrm{inst},m_{s,D}}$ when L is increased through π. When L is increased through 2π, it bifurcates again, into a degenerate pair of unstable states $\pm\phi_{\mathrm{inst},m_{u,D}}$. Unlike the magnetized states, these transition states are positive on half the interval and negative on the other. $m_{u,D}$ is determined from L by the condition $\phi(x = L) = 0$, i.e., by the quarter-period condition $4\sqrt{m_{u,D}+1}\,\mathbf{K}(m_{u,D}) = L$.

The same bifurcation occurs if periodic boundary conditions are used, but the new transition state is infinitely degenerate: it may be shifted by an arbitrary amount. It is easy to see that in the Neumann case, the bifurcation occurs at $L = \pi$ rather than $L = 2\pi$, with the Neumann parameter $m_{u,N}$ determined by a half-period condition. To satisfy Neumann boundary conditions, the field configurations $\pm\phi_{\mathrm{inst},m_{u,N}}$ must be shifted by $L/2$.

Figure 1 displays the magnetized and transition states for each boundary condition. As $L \to \infty$, the Bloch walls between magnetization values increasingly acquire the standard hyperbolic tangent form, since $\mathrm{sn}(\bullet \mid m)$ degenerates to $\tanh(\bullet)$ as $m \to 1^-$.

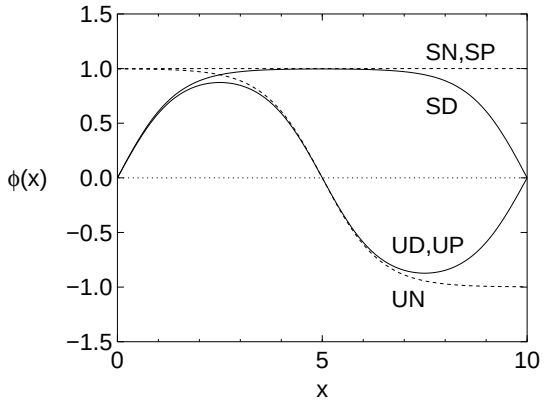

FIG. 1. Stable magnetized states (S) and transition states (U), for Dirichlet (D), Neumann (N), and periodic (P) boundary conditions, if $L = 10$. Each state may be multiplied by -1, and UP may be shifted by an arbitrary amount.

The zero-noise dynamics of the model (1) are of the gradient form $\dot{\phi} = -\delta\mathcal{H}/\delta\phi$, with the energy functional

$$\mathcal{H}[\phi] \equiv \int_0^L \left[(\phi')^2/2 + \left(\phi^2 - 1\right)^2/4\right] dx. \qquad (3)$$

The energy of each magnetized and transition state is readily computed from (3). The states $\phi \equiv \pm 1$ have zero energy, and $\phi \equiv 0$ has energy $L/4$. The energy of each periodic instanton state $\pm\phi_{\mathrm{inst},m}$ turns out to be

$$\frac{L}{12}\left[\frac{8}{(m+1)}\,\frac{\mathbf{E}(m)}{\mathbf{K}(m)} - \frac{(1-m)(3m+5)}{(m+1)^2}\right], \qquad (4)$$

where $\mathbf{E}(m)$ is the second complete elliptic integral [12].

Figure 2 plots the activation barrier ΔW as a function of L, for each boundary condition. Due to the normalization of our model, ΔW equals $2\Delta E$, where ΔE is the energy 'height' of the transition state. The second derivative of each ΔE function is discontinuous at the value of L at which bifurcation occurs. As $L \to \infty$, the value of ΔE converges to the energy of a Bloch wall (Dirichlet, Neumann cases), or two Bloch walls (periodic case). From (3), the energy of a Bloch wall, of the $m \to 1^-$ limiting form $\pm\tanh((x - x_0)/\sqrt{2})$, is $2\sqrt{2}/3 \approx 0.943$.

Determinant Quotients.—The formula for the Kramers rate prefactor Γ_0 of an overdamped multidimensional system driven by white noise is well known. Suppose the system has a stable state $\boldsymbol{\varphi}_s$, and a transition state $\boldsymbol{\varphi}_u$ with a single unstable direction. Let $\boldsymbol{\Lambda}_s$ and $\boldsymbol{\Lambda}_u$ denote the system's linearized noiseless dynamics at $\boldsymbol{\varphi}_s$ and $\boldsymbol{\varphi}_u$, so that to leading order, the state $\boldsymbol{\varphi} = \boldsymbol{\varphi}_s + \boldsymbol{\eta}$ evolves by $\dot{\boldsymbol{\eta}} = -\boldsymbol{\Lambda}_s\boldsymbol{\eta}$, and $\boldsymbol{\varphi} = \boldsymbol{\varphi}_u + \boldsymbol{\eta}$ by $\dot{\boldsymbol{\eta}} = -\boldsymbol{\Lambda}_u\boldsymbol{\eta}$. Then [13]

$$\Gamma_0 = \frac{1}{2\pi}\sqrt{|\Upsilon|}\;|\lambda_{u,1}| \equiv \frac{1}{2\pi}\sqrt{\left|\frac{\det\boldsymbol{\Lambda}_s}{\det\boldsymbol{\Lambda}_u}\right|}\;|\lambda_{u,1}|\,, \qquad (5)$$

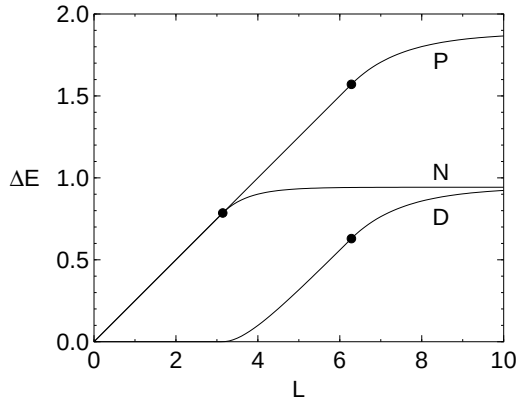

FIG. 2. The energy barrier ΔE, in the cases of Dirichlet (D), Neumann (N), and periodic (P) boundary conditions. Bullets indicate criticality ($L = 2\pi$ for D and P; $L = \pi$ for N).

where $\lambda_{u,1}$ is the only negative eigenvalue of $\mathbf{\Lambda}_u$. The corresponding eigenvector $\boldsymbol{\eta}_{u,1}$ is the direction along which the optimal transition trajectory approaches the transition state. If $\lambda_{s,1}$ denotes the smallest eigenvalue of $\mathbf{\Lambda}_s$, the corresponding eigenvector $\boldsymbol{\eta}_{s,1}$ will be the direction along which the optimal trajectory extends from the stable state.

Linearizing the noiseless version of (1) at a stationary state ϕ_0 (either a stable or a transition state) yields

$$\dot{\eta} = -\hat{\Lambda}[\phi_0]\,\eta \equiv -\left[-d^2/dx^2 + (-1 + 3\phi_0^2)\right]\eta. \qquad (6)$$

So Γ_0 depends on the spectrum of the $\hat{\Lambda}$ operators associated with the stable and transition states. In the Dirichlet case, the formal determinant quotient Υ can be computed by the 'Jacobi method' of Coleman [5,14]. If $L > 2\pi$, let $\eta_{s,*}$ and $\eta_{u,*}$ be the solutions on $[0, L]$ of the homogeneous differential equations $\hat{\Lambda}[\phi_{\mathrm{inst},m_{s,D}}]\eta = 0$ and $\hat{\Lambda}[\phi_{\mathrm{inst},m_{u,D}}]\eta = 0$ which satisfy the boundary conditions $\eta(0) = 0$ and $\eta'(0) = 1$. Then, it turns out that

$$\Upsilon_D \equiv \eta_{s,*}(L)/\eta_{u,*}(L) \qquad (7)$$

is the Dirichlet-case determinant quotient.

Solutions $\eta_{s,*}$ and $\eta_{u,*}$ satisfying these special boundary conditions may be constructed by a clever trick [14]: differentiating the periodic instanton $\phi_{\mathrm{inst},m}$ with respect to m, setting m to $m_{s,D}$ and $m_{u,D}$ respectively, and normalizing. This procedure uses the little-known formula for the derivative of $\mathrm{sn}(\bullet \mid m)$ with respect to m [15]. The result is

$$\eta_{c,*}(L) = \pm\frac{L}{m_{c,D}^2 - m_{c,D} + 1}\left[\frac{m_{c,D}+1}{1-m_{c,D}}\,\frac{\mathbf{E}(m_{c,D})}{\mathbf{K}(m_{c,D})} - 1\right],$$

for $c = s, u$ ('$\pm$' being $+, -$ respectively). Substituting $\eta_{s,*}(L)$ and $\eta_{u,*}(L)$ into (7) yields the quotient Υ_D.

The unbifurcated regime, i.e., $\pi < L < 2\pi$, must be handled a bit differently. Since the transition state in this regime is $\phi \equiv 0$, rather than $\phi_{\mathrm{inst},m_{u,D}}$, the quantity $\eta_{u,*}(L)$ cannot be computed from the above formula. But it is easy to check that $\eta_{u,*}(L)$ simply equals $\sin L$.

The Neumann case is treated similarly to the Dirichlet (we omit the details), but the case of periodic boundary conditions is very different, at least in the bifurcated regime $L > 2\pi$. The periodic instanton transition state is infinitely rather than doubly degenerate, and at any transition state, the linearized dynamical operator $\hat{\Lambda}$ has a soft 'collective mode', with a zero eigenvalue. On account of this mode, Eq. (5) must be modified, but the regularization technique of McKane and Tarlie [14] can be used to work out the periodic-case Kramers prefactor [16]. It acquires an $\epsilon^{-1/2}$ factor, so the reversal rate becomes non-Arrhenius when $L > 2\pi$. This is like the non-Arrhenius reversal rate falloff displayed by the stochastic Landau–Lifshitz–Gilbert equation [3], which is also due to an infinitely degenerate transition state.

The Unstable Eigenvalue.—The stumbling block in the analytic computation of the Dirichlet-case Kramers rate prefactor is the calculation of $\lambda_{u,1}$, the single negative (unstable) eigenvalue of the deterministic dynamics, linearized at the transition state. If $\pi < L < 2\pi$ and $\phi \equiv 0$ is the transition state, then $\lambda_{u,1} = \pi^2/L^2 - 1$ is easy to verify. But computing $\lambda_{u,1}$ and the corresponding eigenfunction $\eta_{u,1}$ when $L > 2\pi$ is far harder. $\eta_{u,1}$ is of considerable physical interest, since it characterizes the way in which the optimal reversal trajectories approach the periodic instanton solutions $\pm\phi_{\mathrm{inst},m_{u,D}}$, i.e., the way in which the moving Bloch wall slows to a halt at $x = L/2$.

Here we sketch the calculation of $\lambda_{u,1}$ and $\eta_{u,1}$ from the eigenvalue equation $\hat{\Lambda}\eta = \lambda\eta$; details will appear elsewhere [16]. Introducing $z \equiv x/\sqrt{m_{u,D}+1}$, and for simplicity, writing m for $m_{u,D}$, converts the equation to

$$\left[-d^2/dz^2 + 6m\,\mathrm{sn}^2(z \mid m)\right]\eta = \mathcal{E}\eta, \qquad (8)$$

where the 'energy' $\mathcal{E}$ equals $(m+1)(\lambda_{u,1}+1)$. The interval $0 \le z \le 4\mathbf{K}(m)$ corresponds to $[0, L]$. Equation (8) is the $l = 2$ Lamé equation [17,18], which is a Schrödinger equation with a periodic potential, whose lattice constant is $2\mathbf{K}(m)$. Its Bloch wave spectrum is known to consist of three energy bands [18], each extending over the wavenumber range $-\pi/2\mathbf{K}(m) \le k \le \pi/2\mathbf{K}(m)$.

According to Hermite's solution of the Lamé equation [19], Eq. (8) has solutions of the form

$$\eta(z) = \prod_{i=1}^{2}\left\{\left[\frac{\mathrm{H}(z \pm \alpha_i \mid m)}{\Theta(z \mid m)}\right]\exp[\mp\,\mathrm{Z}(\alpha_i \mid m)\,z]\right\}, \qquad (9)$$

where H, Θ, and Z are the Jacobi eta, theta, and zeta functions, and α_1, α_2 are complex numbers determined in a complicated way by $\mathcal{E}$. Clearly, the wavenumber k of the solution (9) equals $\pm\mathrm{Im}\sum_{i=1}^{2}\mathrm{Z}(\alpha_i \mid m)$.

The difficulty lies in finding closed-form expressions for α_1, α_2 which will yield a solution $\eta = \eta_{u,1}(z)$ that satisfies Dirichlet boundary conditions on $0 \le z \le 4\mathbf{K}(m)$. But $\eta_{u,1}$, being a ground state, must have no nodes. It should extend

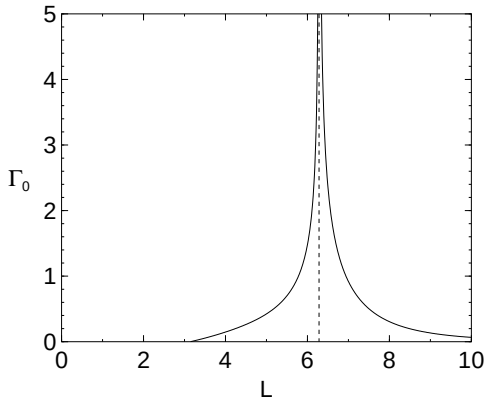

FIG. 3. The Kramers rate prefactor Γ_0 in the Dirichlet case.

to a periodic function with period $8\mathbf{K}(m)$, so its wavenumber must be $\pm\pi/4\mathbf{K}(m)$. Maier [20] has found expressions for α_1, α_2 in terms of $\mathcal{E}$, which yield a closed-form dispersion relation $\mathcal{E} \mapsto \pm k$. By inverting this numerically, we obtain an energy $\mathcal{E}$ corresponding to $k = \pm\pi/4\mathbf{K}(m)$, and hence the eigenvalue $\lambda_{u,1}$.

The Prefactor.—The Dirichlet-case Kramers rate prefactor Γ_0 can be computed from the formula (5), using the closed-form expression (7) for the determinant quotient, and the just-explained technique of calculating the unstable eigenvalue $\lambda_{u,1}$. Figure 3 shows the dependence of Γ_0 on the interval length L. The divergence at $L = 2\pi$, which is caused by a divergence of the determinant quotient, is typical of a second-order phase transition.

The marked asymmetry is partly due to there being two transition states if $L > 2\pi$. But the divergence can be attributed to the bifurcation of the optimal reversal trajectory, rather than to the bifurcation of its endpoint. A two-dimensional nonequilibrium model, whose optimal transition trajectory bifurcates but whose transition state does not, has a similar prefactor divergence [21].

In more complicated field theories perturbed by spatio-temporal noise, such phase transitions may be first-order rather than second-order, with a discontinuous, rather than diverging, prefactor. Kuznetsov and Tinyakov [10] have studied stationary field configurations in a sixth-degree Ginzburg–Landau model, with $\phi + \alpha\phi^3 - (\alpha+1)\phi^5$ replacing the $\phi - \phi^3$ terms of (1). If $\alpha > -1$, the periodic instanton branch of $L \mapsto \Delta E$, the energy barrier function, crosses the $\phi \equiv 0$ sphaleron branch at a nonzero angle. This should give rise to a first-order transition. So, in the (L, α) plane, the second-order transition point $(2\pi, -1)$ must be the endpoint of a first-order transition curve.

Conclusion.—In simple one-dimensional models of magnetization reversal induced by weak noise, taking finite spatial extent and boundary conditions into account yields a rich structure of activation regimes separated by phase transitions. The generality of our approach suggests that spatially extended noise-perturbed systems, whether magnetic or not, should display similar phase transitions. By definition, these will only be accessible to theoretical techniques adapted to finite-size systems.

This research was partially supported by NSF grants PHY-9800979 and PHY-0099484.

[1] J. García-Ojalvo and J. M. Sancho, *Noise in Spatially Extended Systems* (Springer, New York/Berlin, 1999).
[2] G. Brown, M. A. Novotny, and P. A. Rikvold, J. Appl. Phys. **87**, 4792 (2000).
[3] E. D. Boerner and H. N. Bertram, IEEE Trans. Magnetics **34**, 1678 (1998).
[4] U. Bisang and G. Ahlers, Phys. Rev. Lett. **80**, 3061 (1998); Y. Tu, Phys. Rev. E **56**, R3765 (1997).
[5] L. S. Schulman, *Techniques and Applications of Path Integration* (Wiley, New York, 1981), chapter 29.
[6] (a) H.-B. Braun, Phys. Rev. Lett. **71**, 3557 (1993); Phys. Rev. B **50**, 16501 (1994). (b) H.-B. Braun and H. N. Bertram, J. Appl. Phys. **75**, 4609 (1994).
[7] J. S. Langer, Ann. Physics **41**, 108 (1967).
[8] W. G. Faris and G. Jona-Lasinio, J. Phys. A **15**, 3025 (1982). For later work, see F. Martinelli, E. Olivieri, and E. Scoppola, J. Stat. Phys. **55**, 477 (1989).
[9] E. M. Chudnovsky, Phys. Rev. A **46**, 8011 (1992); K. L. Frost and L. G. Yaffe, Phys. Rev. D **59**, 065013 (1999).
[10] A. N. Kuznetsov and P. G. Tinyakov, Phys. Lett. B **406**, 76 (1997).
[11] J. A. Espichán Carrillo, A. Maia, Jr., and V. M. Mostepanenko, Int. J. Mod. Phys. A **15**, 2645 (2000).
[12] *Handbook of Mathematical Functions*, edited by M. Abramowitz and I. A. Stegun (Dover, New York, 1965); R. H. Good, Eur. J. Phys. **22**, 119 (2001).
[13] P. Hänggi, P. Talkner, and M. Borkovec, Rev. Mod. Phys. **62**, 251 (1990).
[14] A. J. McKane and M. B. Tarlie, J. Phys. A **28**, 6931 (1995).
[15] E. H. Neville, *Jacobian Elliptic Functions*, 2nd ed. (Oxford University Press, Oxford, 1951), chapter XV.
[16] R. S. Maier and D. L. Stein, in preparation.
[17] B. J. Harrington, Phys. Rev. D **18**, 2982 (1978).
[18] H. Li, D. Kusnezov, and F. Iachello, J. Phys. A **33**, 6413 (2000).
[19] E. T. Whittaker and G. N. Watson, *A Course of Modern Analysis*, 4th ed. (Cambridge University Press, Cambridge, UK, 1927), section 23.71.
[20] R. S. Maier, in preparation.
[21] R. S. Maier and D. L. Stein, J. Stat. Phys. **83**, 291 (1996). The prefactor divergence is plotted in Fig. 5.